ESC HEART FAILURE
ESC Heart Failure 2020; **7**: 2838–2852
Published online 14 July 2020 in Wiley Online Library (wileyonlinelibrary.com) **DOI:** 10.1002/ehf2.12887

ORIGINAL RESEARCH ARTICLE

Modulation of the acute defence reaction by eplerenone prevents cardiac disease progression in viral myocarditis

Carsten Tschöpe[1,2,3]*, Sophie Van Linthout[1,2], Sebastian Jäger[4], Robert Arndt[5], Tobias Trippel[3], Irene Müller[1,2], Ahmed Elsanhoury[1,2], Susanne Rutschow[6], Stefan D. Anker[1,2,3], Heinz-Peter Schultheiss[7], Matthias Pauschinger[8], Frank Spillmann[3] and Kathleen Pappritz[1,2]

[1]*Berlin Institute of Health Center for Regenerative Therapies and Berlin-Brandenburg Center for Regenerative Therapies (BCRT), Charité—Universitätsmedizin Berlin, Berlin, Germany;* [2]*German Center for Cardiovascular Research (DZHK), Partner site Berlin, Berlin, Germany;* [3]*Department of Cardiology, Charité—Universitätsmedizin Berlin, Campus Virchow Klinikum (CVK), Berlin, Germany;* [4]*Department of Cardiology, Alexianer Hospital Hedwigshöhe, Berlin, Germany;* [5]*Department of Emergency Medicine, Charité—Universitätsmedizin Berlin, Campus Benjamin Franklin (CBF), Berlin, Germany;* [6]*Department of Cardiology, Angiology Johanniter-Kliniken, Stendal, Germany;* [7]*Institute for Cardiac Diagnostics and Therapy (IKDT), Berlin, Germany;* [8]*Department of Cardiology, Paracelsus University, Klinikum Nürnberg, Nürnberg, Germany*

Abstract

Aims Left ventricular (LV) dysfunction in viral myocarditis is attributed to myocardial inflammation and fibrosis, inducing acute and long-time cardiac damage. Interventions are not established. On the basis of the link between inflammation, fibrosis, aldosterone, and extracellular matrix regulation, we aimed to investigate the effect of an early intervention with the mineralocorticoid receptor antagonist (MRA) eplerenone on cardiac remodelling in a murine model of persistent coxsackievirus B3 (CVB3)-induced myocarditis.

Methods and results SWR/J mice were infected with 5×10^4 plaque-forming units of CVB3 (Nancy strain) and daily treated either with eplerenone (200 mg/kg body weight) or with placebo starting from Day 1. At Day 8 or 28 post infection, mice were haemodynamically characterized and subsequently sacrificed for immunohistological and molecular biology analyses. Eplerenone did not influence CVB3 load. Already at Day 8, 1.8-fold ($P < 0.05$), 1.4-fold ($P < 0.05$), 3.2-fold ($P < 0.01$), and 2.1-fold ($P < 0.001$) reduction in LV intercellular adhesion molecule 1 expression, presence of monocytes/macrophages, oxidative stress, and apoptosis, respectively, was observed in eplerenone-treated vs. untreated CVB3-infected mice. *In vitro*, eplerenone led to 1.4-fold ($P < 0.01$) and 1.2-fold ($P < 0.01$) less CVB3-induced cardiomyocyte oxidative stress and apoptosis. Furthermore, collagen production was 1.1-fold ($P < 0.05$) decreased in cardiac fibroblasts cultured with medium of eplerenone-treated vs. untreated CVB3-infected HL-1 cardiomyocytes. These ameliorations were *in vivo* translated into prevention of cardiac fibrosis, as shown by 1.4-fold ($P < 0.01$) and 2.1-fold ($P < 0.001$) lower collagen content in the LV of eplerenone-treated vs. untreated CVB3-infected mice at Days 8 and 28, respectively. This resulted in an early and long-lasting improvement of LV dimension and function, as indicated by reduced LV end-systolic volume and end-diastolic volume, and an increase in LV contractility (dP/dt_{max}) and LV relaxation (dP/dt_{min}), respectively ($P < 0.05$).

Conclusions Early intervention with the MRA eplerenone modulates the acute host and defence reaction and prevents cardiac disease progression in experimental CVB3-induced myocarditis without aggravation of viral load. The findings advocate for an initiation of therapy of viral myocarditis as early as possible, even before the onset of inflammation-induced myocardial dysfunction. This may also have implications for coronavirus disease-19 therapy.

Keywords Myocarditis; Mineralocorticoid receptor inhibition; Inflammation; Fibrosis; Coxsackievirus B3; COVID-19

Received: 14 April 2020; Revised: 4 June 2020; Accepted: 24 June 2020
**Correspondence to: Carsten Tschöpe, Berlin Institute of Health Center for Regenerative Therapies (BCRT), Charité—Universitätsmedizin Berlin, CVK, Föhrer Strasse 15, D-13353 Berlin, Germany. Tel: 0049 30 450553712; Fax: 0049 30 450565900. Email: carsten.tschoepe@charite.de*
Carsten Tschöpe and Sophie Van Linthout contributed equally to this work.

Introduction

Myocarditis is most commonly of viral aetiology[1,2] and is histopathologically characterized by an infiltration of inflammatory cells into the myocardium accompanied by degeneration of cardiomyocytes and the extracellular matrix (ECM).[3,4] Numerous viruses, including adenoviruses, herpes viruses, enteroviruses including coxsackievirus B3 (CVB3), cytomegaloviruses, human immunodeficiency virus, parvovirus B19, and probably hepatitis C, influenza, and coronaviruses, are associated with myocarditis in humans.[1,5,6] Especially, infections with CVB3 are a known cause of acute and fulminant viral myocarditis in young, otherwise healthy patients.[7] Both direct viral cytotoxic and immune-mediated mechanisms after CVB3 infection contribute to myocyte injury and result in cardiac dysfunction.[8,9] A significant proportion of patients who recover from acute myocarditis eventually develop dilated cardiomyopathy, leading to severe heart failure and ultimately requiring heart transplantation.[10–13] Progression of the disease is not only attributed to viral persistence and a chronic inflammatory response but also to a profound alteration of ECM structure and the development of cardiac fibrosis.[4,14] Dysregulation in ECM production and degradation contributes to the development of a dilative cardiac phenotype, including cardiac scaring, which belongs to an independent risk factor for impaired prognosis, even in myocarditis.[15] A panel of different (anti-)inflammatory and (anti-)fibrotic network systems including macrophages, B and T cells,[8,16–18] platelets,[19] myofibroblasts,[20,21] cytokines,[22–24] chemokines,[25] damage-associated molecular patterns,[26–30] soluble ST2,[31] lysyl oxidase-like 2,[18] galectin-3,[32] matrix metalloproteinases (MMPs) and their tissue inhibitors (TIMP)[33,34] as well as aldosterone,[24,35] play a major role in the defence and healing process under these circumstances. For most of these potential targets, with the exception of aldosterone, no well-established therapeutic strategies are available, and no direct translation into the clinic is possible.[36] In an animal study, aldosterone infusion has been shown to induce ventricular hypertrophy and interstitial fibrosis in both right and left ventricles.[37] Further studies have suggested that aldosterone-induced generation of reactive oxygen species and low-grade inflammation underlie aldosterone-induced cardiac fibrosis.[38,39] With respect to acute myocarditis, a significant increased intramyocardial aldosterone synthesis has been found in the myocardium of patients with biopsy-proven acute myocarditis.[40] Because an uncontrolled early fulminant activated immune reaction together with aldosterone can trigger an irreversible cardiac damage with long-time consequences for cardiac remodelling and function in the post-inflammatory myocarditis phase, we sought to demonstrate whether an early intervention with the mineralocorticoid receptor antagonist (MRA) eplerenone (EPL) exerts cardio-beneficial effects to balance the inflammatory defence and healing reaction of the immune system in a murine model of persisting CVB3-induced myocarditis. This research may also have implications for viral heart disease due to the severe acute respiratory syndrome coronavirus 2, that is, in association with coronavirus disease-19 (COVID-19).[5,41]

Methods

Animal model of virus-induced myocarditis

Five to six weeks old, male SWR/J mice (Jackson Laboratory, Bar Harbor, ME, USA) were maintained under standard housing conditions (12 h light/dark cycle, temperature 22 ± 2°C) and received water and food *ad libitum*. On Day 0, half of the mice were either infected with 5×10^4 plaque-forming units (p.f.u.) CVB3 (Nancy strain) dissolved in 0.2 mL of saline or sham-infected with 0.2 mL of saline by intraperitoneal (i.p.) injection. On the first day post infection (p.i.), half of each group was randomly assigned to receive either EPL [200 mg/kg body weight (BW) dissolved in 0.2 mL of water] or placebo (0.2 mL of water) by daily gavage. Haemodynamic measurements were performed on Day 8 or 28 p.i. All investigations were performed in accordance with the 'Guide for the Care and Use of Laboratory Animals' published by the US National Institutes of Health (NIH publ. no. 85-23, revised 1985).

Haemodynamic measurement

Mice were anaesthetized with thiopental (125 μg/g BW i.p.), intubated, and artificially ventilated. LV end-systolic pressure (in mmHg), the maximal rate of LV pressure rise (dP/dt_{max}; in mmHg/s), LV end-diastolic pressure (in mmHg), the minimal rate of LV pressure fall (dP/dt_{min}; in mmHg/s), and end-systolic and end-diastolic volume (μL) were recorded via a conductance catheter (1.4 French; Millar, Houston, TX, USA) system in closed-chest animals, as described previously.[42,43]

Tissue preparation

After haemodynamic measurements, animals were euthanized. The LV was dissected, snap-frozen in liquid nitrogen, and stored at −80°C until further molecular analyses. Transverse LV sections were either embedded in Tissue Tek (Sakura, Tokyo, Japan) for immunohistological staining or fixed in 4% buffered formalin and subsequently embedded in paraffin for picrosirius red staining.

Gene expression analysis

LV tissue samples were homogenized, and total RNA was extracted using the TRIzol reagent (Invitrogen, Carlsbad, California, USA) and further purified using the RNeasy-Kit (Qiagen, Hilden, Germany). Purified RNA was reverse transcribed into cDNA using the high capacity kit (Applied Biosystems, Foster City, CA, USA). Quantitative real-time PCR was performed on an ABI PRISM 7700 sequence detection system (Applied Biosystems, Foster City, CA, USA) using TaqMan universal master mix and TaqMan gene expression assays [connective tissue growth factor (cTGF), Mm01192931_g1; Col1a1, Mm01302043_g1; Col3a1, Mm01254467_m1; transforming growth factor (TGF)-β, Mm00436955_m1; interleukin (IL)-6, Mm00446190_m1; tumour necrosis factor (TNF)-α, Mm00443258 _m1; MMP-3, Mm01168406_g1; MMP-8, Mm00772335_m1; MMP-12, Mm00500554_m1; MMP-13, Mm01168713_m1; TIMP-1, Mm01341361_m1; TIMP-2, Mm00441825_m1; TIMP-4: Mm00446568_m1]. Viral load was detected via a forward primer (5′-CCCTGAATGCGGCTAA TCC-3′), reverse primer (5′-ATTGTCACCATAAGCAGCCA-3′), and FAM-labelled MGB probe (FAM 5′-TGCA GCGGAACCG-3′). Expression of the respective target gene was normalized to the housekeeping gene 18s (Hs99999901_s1) using the $2^{\Delta Ct}$ method.[44]

Picrosirius red staining

To quantify total myocardial collagen content, picrosirius red staining (Polyscience, Inc., Warrington, PA, USA) was performed, as previously described.[45] The stained sections were investigated under circularly polarized light by using digital image analysis. In general, >20 fields at a 200-fold magnification were analysed, and total collagen content was measured [positive area fraction (AF) in %]. Perivascular fibrosis was excluded from the measurement.

Immunohistology

As described previously,[46] immunohistological stainings were performed using the indirect method by incubation with a specific primary antibody, subsequent incubation with an appropriate secondary antibody, and final visualization by a horseradish peroxidase reaction. Anti-CD11b (Pharmingen, San Diego, CA, USA) followed by DAKO EO 468 (DAKO, Glostrup, Denmark) was used to quantify CD11b-positive cells/heart area (HA). Anti-intercellular adhesion molecule (anti-ICAM)-1 (Pharmingen, San Diego, CA, USA) in combination with Dianova #127-035-160 (Dianova, Hamburg, Germany), and anti-collagen I (Chemicon, Billerica, MA, USA), anti-collagen III (Calbiochem, Darmstadt, Germany), and anti-nitrotyrosine (Sigma-Aldrich, St. Luis, MO, USA) in combination with EnVision-anti-rabbit (DAKO, Glostrup, Denmark) was used to determine LV immune cell infiltration, fibrosis, and oxidative stress as AF or number of cells/HA.

Matrix metalloproteinase-2 and matrix metalloproteinase-9 zymography

Gelatin zymography was used to assess the activity of MMP-2 and MMP-9. Therefore, purified LV protein samples (40 μg) were mixed with sample buffer [10% w/v sodium dodecyl sulfate (SDS), 4% w/v sucrose, and 0.1% w/v bromophenol blue] in a final volume of 20 μL. Proteins were separated in a 10% polyacrylamide gel containing 0.1% gelatin. After staining with coomassie G250 and destaining in 7% acetic acid/35% methanol, gelatinolytic activity could be visualized as clear bands in the gel. The scanned bands of active MMP-2 and MMP-9 were densitometrically quantified using Gel-Pro Analyzer 4.0 (Media Cybernetics, Bethesda, MD, USA).

Terminal deoxynucleotidyl transferase-mediated dUTP nick-end labelling assay

To detect apoptosis, the DeadEnd colorimetric terminal deoxynucleotidyl transferase-mediated dUTP nick-end labelling (TUNEL) system (Promega, Madison, WI, USA) was used according to the manufacturer's instructions. Rate of apoptotic myocytes was examined by digital image analysis and expressed as positive cells/HA.

Cell culture

HL-1 cells were plated in a six-well plate or in a 96-well plate at a density of 250 000 cells/well or 10 000 cells/100 μL/well, respectively, in Claycomb medium (Sigma, Steinheim, Germany) supplemented with 10% foetal bovine serum, 1% penicillin/streptomycin, 100 μM of norepinephrine (Sigma), and 2 mM and L-glutamine. After 24 h of culture, cells were serum starved or incubated with CVB3 at a multiplicity of infection of 5 for 1 h. Four hours after CVB3 infection or serum starvation, medium was exchanged by 'full' Claycomb medium containing 0 or 3 μM of EPL. Twenty-four hours after infection or serum starvation, cells in the six-well were collected for reactive oxygen species (ROS) analysis by flow cytometry. Caspase 3/7 activity was measured in the 96-well plate or medium from the cells plated in the 96-well plate (control; EPL; CVB3; and CVB3/EPL) was collected and frozen at −80°C until further culture on cardiac fibroblasts.

Cardiac fibroblasts (7500/well) were plated in a 96-well plate at a density of 7500 cells/well in Lung/Cardiac Fibroblasts Basal Medium (Cell Applications, Inc., San Diego, USA) plus supplements (Cell Applications). After 24 h of culture,

medium was removed, two times washed with phosphate-buffered saline (PBS), and supplemented for 24 h with control, EPL, CVB3, or CVB3/EPL medium collected from HL-1 cells. Next, Sirius Red and crystal violet staining was performed.

Reactive oxygen species analysis

Oxidative stress in HL-1 cells was determined via analysis of ROS by 5-(and-6)-chloromethyl-2′,7′-dichlorodihydrofluorescein diacetate, acetyl ester (CM-H-$_2$DCFDA) (Invitrogen) flow cytometry. Twenty-four hours after CVB3 infection, cells were collected and resuspended in PBS for flow cytometry on a MACSQuant Analyzer (Miltenyi Biotec, Bergisch Gladbach, Germany). DCF+ cells were analysed with FlowJo 8.7 software (Tree Star). Data are expressed as DCF+ cells (% gated).

Caspase 3/7 activity assay

Twenty-four hours after infection or serum starvation, caspase 3/7 activity was determined with a Caspase Glo 3/7 activity kit (Promega) according to the manufacturer's protocol. Luminescence was measured with a luminometer (Berthold Technologies, LB 940 Multimode Reader Mithras, Bad Wildbad, Germany).

Analysis of collagen production in cultured cardiac fibroblasts

Collagen production in human cardiac fibroblasts was determined via Sirius Red staining described previously,[47] followed by normalization to cell number via crystal violet staining. In brief, cardiac fibroblasts were fixed in methanol overnight at −20°C, washed once with PBS, and incubated in 0.1% Direct Red 80 (Sirius red) staining solution at room temperature (RT) for 60 min. After second washing with PBS, the Sirius Red staining of the human cardiac fibroblast was eluted in 0.1 N of sodium hydroxide at RT for 60 min on a rocking platform. The optical density representative for the accumulation of collagen I and III was measured at 540 nm. For crystal violet staining, cardiac fibroblasts were fixed overnight with 4% paraformaldehyde. After the cells were washed with distilled H_2O three times, they were stained with crystal violet solution (Sigma-Aldrich, Steinheim, Germany). After three washing steps with distilled H_2O, cells were incubated with 1% SDS for 1 h. Absorbance was determined at 595 nm. Collagen production in cardiac fibroblasts is depicted as arbitrary units representing the absorbance of Sirius Red staining divided by the mean of the absorbance of crystal violet staining.

Statistical analysis

All data are expressed at mean ± standard error of mean (SEM). Data were tested for normal distribution using the Shapiro–Wilk test. For normal distributed data, ordinary one-way ANOVA and Fisher's least significant difference *post hoc* test was performed. By non-equal standard deviations, Brown–Forsythe and Welch–ANOVA followed by unpaired *t*-test with Welch's correction were performed. In case of the viral load, the CVB3 vs. CVB3/EPL groups were analysed via a Student *t*-test or Mann–Whitney test. Values of $P < 0.05$ were considered significant (Graph Pad Prism 8.0; GraphPad Software, La Jolla, USA).

Results

Eplerenone ameliorates left ventricular function in coxsackievirus B3-induced myocarditis

CVB3 infection caused a progressive LV dilatation, as indicated by an increased end-systolic and end-diastolic volume (*Figure 1A–D*). In parallel, CVB3-infected mice displayed a severely impaired systolic and diastolic LV function, as indicated by reduced dP/dt_{max} (LV contractility; *Figure 1*E and F) and dP/dt_{min} (LV relaxation; *Figure* 1G and H), as compared with control animals. EPL treatment in CVB3 lowered LV dimensions after viral infection vs. vehicle treatment, which was paralleled by ameliorated LV contractility and LV relaxation in CVB3/EPL animals.

Eplerenone does not influence viral load in coxsackievirus B3-induced myocarditis

This impairment in cardiac function after CVB3 infection was further associated with an increased viral load (*Figure 2*). Interestingly, the amelioration of LV function in CVB3/EPL was not accompanied by a decrease in CVB3 mRNA expression.

Eplerenone leads to less immune cell infiltration in coxsackievirus B3-induced myocarditis

Analysis of pro-inflammatory cytokine expression revealed no differences in IL-6 and TNF-α mRNA levels at Days 8 and 28 after CVB3 infection (*Figure 3*). In contrast, protein content of ICAM-1 was found to be noticeably increased in the myocardium of CVB3-infected mice (*Figure 4A and B*), whereas EPL resulted in a significant reduction of ICAM-1 protein content. Correspondingly, we observed a markedly increased presence of monocytes/macrophages into the myocardium of infected mice, as assessed by immunohistochemical staining for $CD11b^+$ cells (*Figure* 4C and B). In comparison with the

FIGURE 1 Eplerenone improves left ventricular (LV) function in coxsackievirus B3-induced myocarditis. Eight and 28 days after CVB3 infection, mice were haemodynamically characterized via conductance catheter measurements. In detail, LV dimensions, indicated by LV end-systolic (LVESV; A and B) and end-diastolic volume (LVEDV; C and D) and cardiac contractility (dp/dt_{max}; E and F) and relaxation (dp/dt_{min}; G and H) were determined. Data are reported as mean ± SEM and were analysed with one-way ANOVA and Fisher's least significant difference (LSD) *post hoc* test or Welch–ANOVA (*P < 0.05, **P < 0.01; ***P < 0.001; ****P < 0.0001 with n = 5–8/group). CVB3, coxsackievirus B3; d, days; EPL, eplerenone; p.i., post infection.

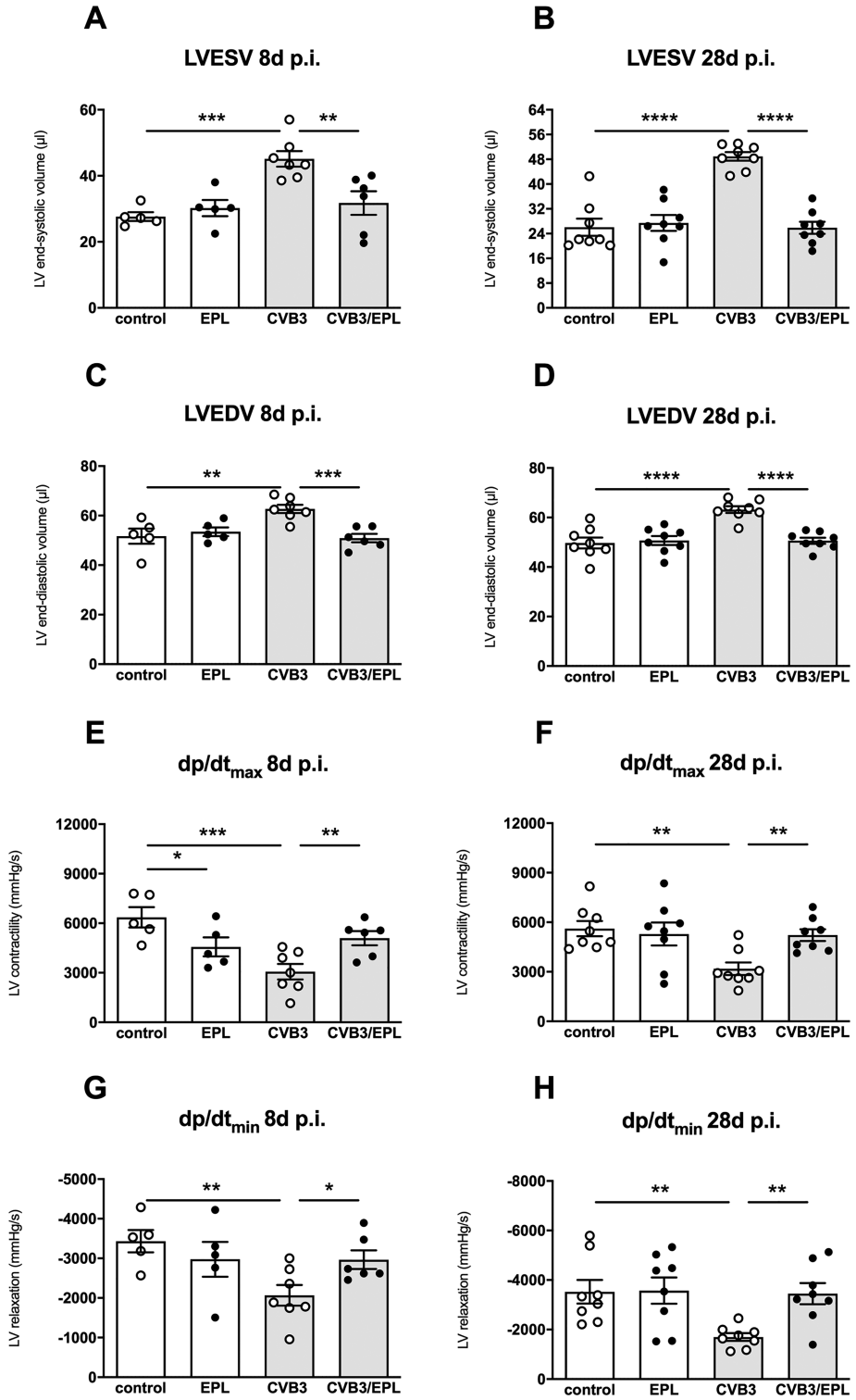

DOI: 10.1002/ehf2.12887

FIGURE 2 Eplerenone does not reduce viral load in coxsackievirus B3-induced myocarditis. Left ventricular (LV) viral load was determined by gene expression analysis in mice, 8 and 28 days after saline injection or CVB3 infection. Data are reported as mean ± SEM and were analysed with Student *t*-test or Mann–Whitney test (*$P < 0.05$, **$P < 0.01$; ***$P < 0.001$; ****$P < 0.0001$ with $n = 8$/group). CVB3, coxsackievirus B3; d, days; EPL, eplerenone; p.i., post infection.

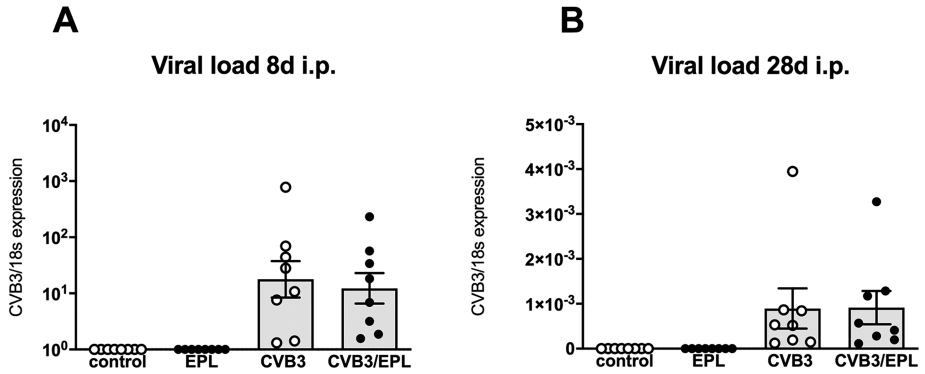

FIGURE 3 Eplerenone does not affect left ventricular gene expression of inflammatory cytokines in coxsackievirus B3-induced myocarditis. Gene expression of pro-inflammatory cytokines interleukin (IL)-6 (A and B), and tumour necrosis factor (TNF)-α at 8 days (left panels), and 28 days (right panels) after saline injection or CVB3 infection. Data are reported as mean ± SEM and were analysed with one-way ANOVA and Fisher's least significant difference (LSD) *post hoc* test or Welch–ANOVA (*$P < 0.05$; **$P < 0.01$; ***$P < 0.001$; ****$P < 0.0001$ with $n = 7$–8/group). CVB3, coxsackievirus B3; d, days; EPL, eplerenone; p.i., post infection.

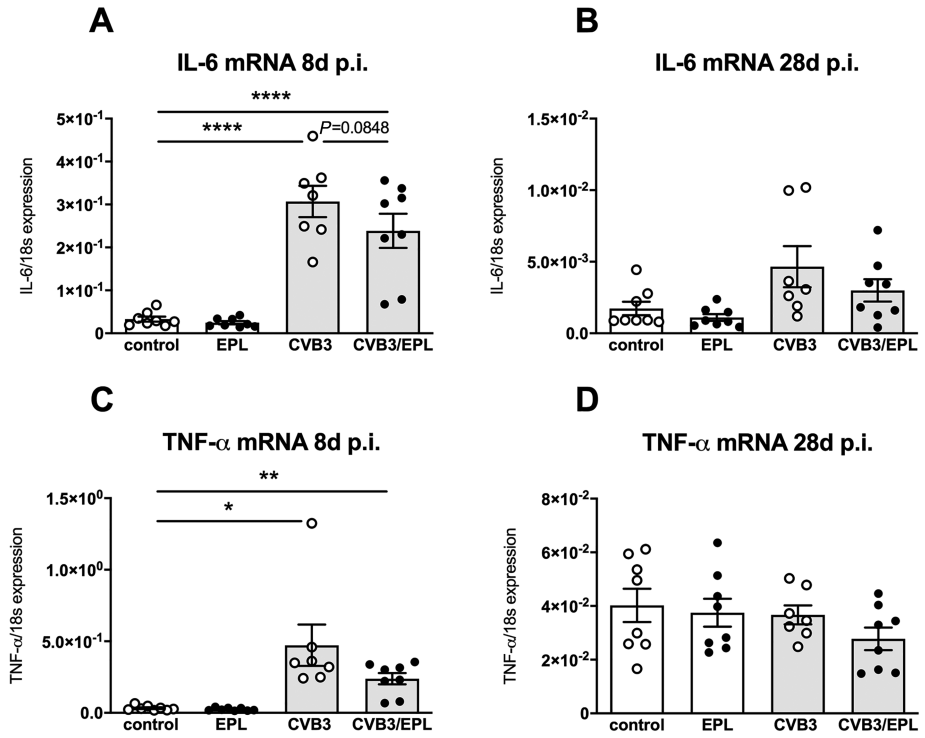

DOI: 10.1002/ehf2.12887

FIGURE 4 Eplerenone leads to less immune cell infiltration in coxsackievirus B3-induced myocarditis. Immunohistochemical analysis of intercellular adhesion molecule (ICAM)-1 protein expression (A and B). Number of CD11b$^+$ cells (C and D) was assessed to determine monocyte/macrophage presence. Representative pictures (magnification 200-fold) of left ventricular (LV) sections from control, CVB3, and CVB3/EPL mice, at Days 8 and 28 after saline injection or CVB3 infection are depicted. Quantitative analysis was performed via digital image analysis and expressed as positive area fraction (%) or number of cells/heart area (HA; mm^2). Data are reported as mean ± SEM and were analysed with one-way ANOVA and Fisher's least significant difference (LSD) *post hoc* test or Welch–ANOVA (*P < 0.05, **P < 0.01; ***P < 0.001; ****P < 0.0001 with n = 8/group). CVB3, coxsackievirus B3; d, days; EPL, eplerenone; p.i., post infection.

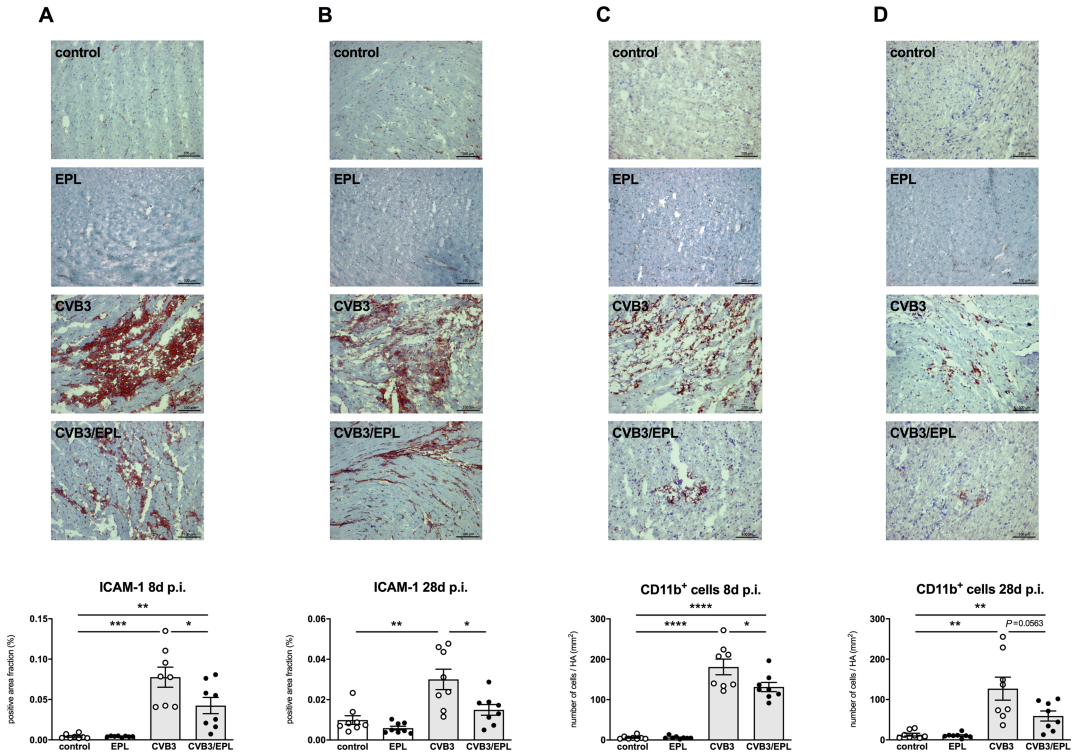

CVB3 group, EPL led to a significant reduction of monocytes/macrophages in CVB3/EPL mice.

Eplerenone abrogates oxidative stress and prevents cardiomyocyte apoptosis in coxsackievirus B3-induced myocarditis

Oxidative stress in the LV was quantified by immunohistochemical staining for nitrotyrosine (*Figure 5A–D*). We observed an enhanced positive AF for nitrotyrosine 8 days p.i., which was prevented by EPL. However, no significant changes in nitrotyrosine staining were detected in any group at 28 days p.i. *In vitro*, EPL decreased the oxidative stress, depicted as DCF+ cells, in CVB3-infected HL-1 cardiomyocytes (*Figure* 5E).

TUNEL assay revealed an increase of apoptotic cardiomyocytes at Day 8 p.i. as compared with those in the respective control group (*Figure* 5F and G). This increase was significantly attenuated by EPL. An up-regulated apoptosis rate was also detected 28 days p.i., while EPL-treated animals displayed a reduction of apoptotic cells to control level. Supplementation of EPL to CVB3-infected HL-1 cardiomyocytes decreased the CVB3-induced apoptosis as indicated by lower caspase 3/7 activity compared with non-treated CVB3-infected HL-1 (*Figure* 5H).

Eplerenone attenuates interstitial myocardial fibrosis in coxsackievirus B3-induced myocarditis

Gene expression of Col1a1, Col3a1, cTGF, and TGF-β was increased in the myocardium of CVB3-infected mice at 8 days p.i. (*Figure S1*). EPL attenuated the expression of Col1a1, Col3a1, and cTGF in CVB3/EPL animals vs. CVB3 mice (*Figure S1*). Picrosirius red staining demonstrated a progressive interstitial myocardial fibrosis in CVB3-infected mice vs. control at both time points (*Figure 6A–D*), which was significantly

FIGURE 5 Eplerenone abrogates oxidative stress and prevents cardiomyocyte apoptosis in coxsackievirus B3-induced myocarditis. Nitrotyrosine staining (A–D) in the heart was performed to assess oxidative stress. Representative pictures (magnification 200-fold) of left ventricular (LV) sections from control, CVB3, and CVB3/EPL mice at Days 8 and 28 after saline injection or CVB3 infection are depicted. In parallel, oxidative stress was detected in HL-1 cardiomyocytes via DCF staining. Data are represented as DCF+ cells (% gated cells; E). In addition, LV cardiomyocyte apoptosis (F and G) was evaluated by terminal deoxynucleotidyl transferase-mediated dUTP nick-end labelling (TUNEL) staining in control, CVB3, and CVB3/EPL mice at Days 8 and 28 after saline injection or CVB3 infection. Evaluation of apoptosis in HL-1 cardiomyocytes was performed via measurement of caspase 3/7 activity depicted as RLU (relative light units; H). Data are reported as mean ± SEM and were analysed with one-way ANOVA and Fisher's least significant difference (LSD) *post hoc* test or Welch–ANOVA (*P < 0.05, **P < 0.01; ***P < 0.001; ****P < 0.0001 with n = 8/group *in vivo* and n = 5–7/group for DCF flow cytometry and n = 6/group for caspase 3/7 measurements). CVB3, coxsackievirus B3; d, days; EPL, eplerenone; HA, heart area; p.i., post infection; ROS, reactive oxygen species; TUNEL, terminal deoxynucleotidyl transferase-mediated dUTP nick-end labelling.

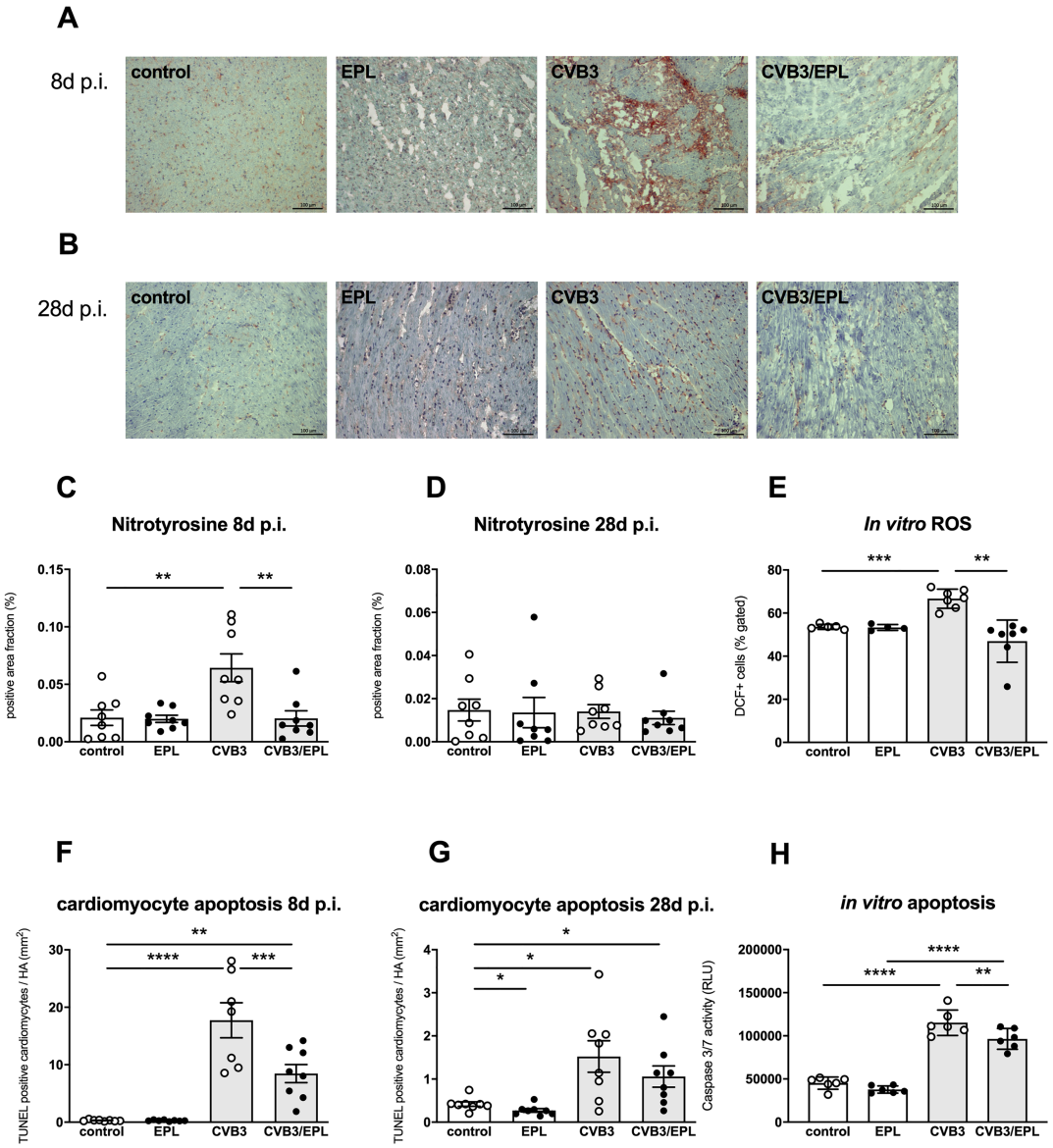

attenuated by EPL. Interestingly, immunohistochemistry revealed that collagen type I content was significantly increased in infected mice compared with controls (*Figure 6E and F*), whereas collagen type III content remained unchanged (*Figure 6G and H*). Application of EPL in CVB3 mice reduced the LV content of collagen type I vs. vehicle-treated CVB3 mice. *In vitro*, cardiac fibroblasts cultured with medium of CVB3-infected HL-1 cardiomyocytes produced more collagen than did those cultured with medium of non-infected HL-1. In contrast, collagen production was less pronounced in cardiac fibroblasts cultured with medium of CVB3/EPL vs. CVB3 HL-1 medium (*Figure* 7).

DOI: 10.1002/ehf2.12887

FIGURE 6 Eplerenone attenuates total collagen content expression in coxsackievirus B3-induced myocarditis. Total collagen content of LV transverse sections was investigated with picrosirius red staining on paraffin sections. Representative pictures at 8 (A) and 28 (B) days after saline of CVB3 infection were shown at a 200-fold magnification. Quantitative analysis (C and D) was performed via digital image analysis and expressed as positive area fraction (%). In addition, cardiac collagen type I (E and F) and type III (G and H) were determined on cryosections at both time points. Data are reported as mean ± SEM and were analysed with one-way ANOVA and Fisher's least significant difference (LSD) *post hoc* test or Welch–ANOVA (**P* < 0.05, ***P* < 0.01; ****P* < 0.001; *****P* < 0.0001 with *n* = 8/group). CVB3, coxsackievirus B3; d, days; EPL, eplerenone; p.i., post infection.

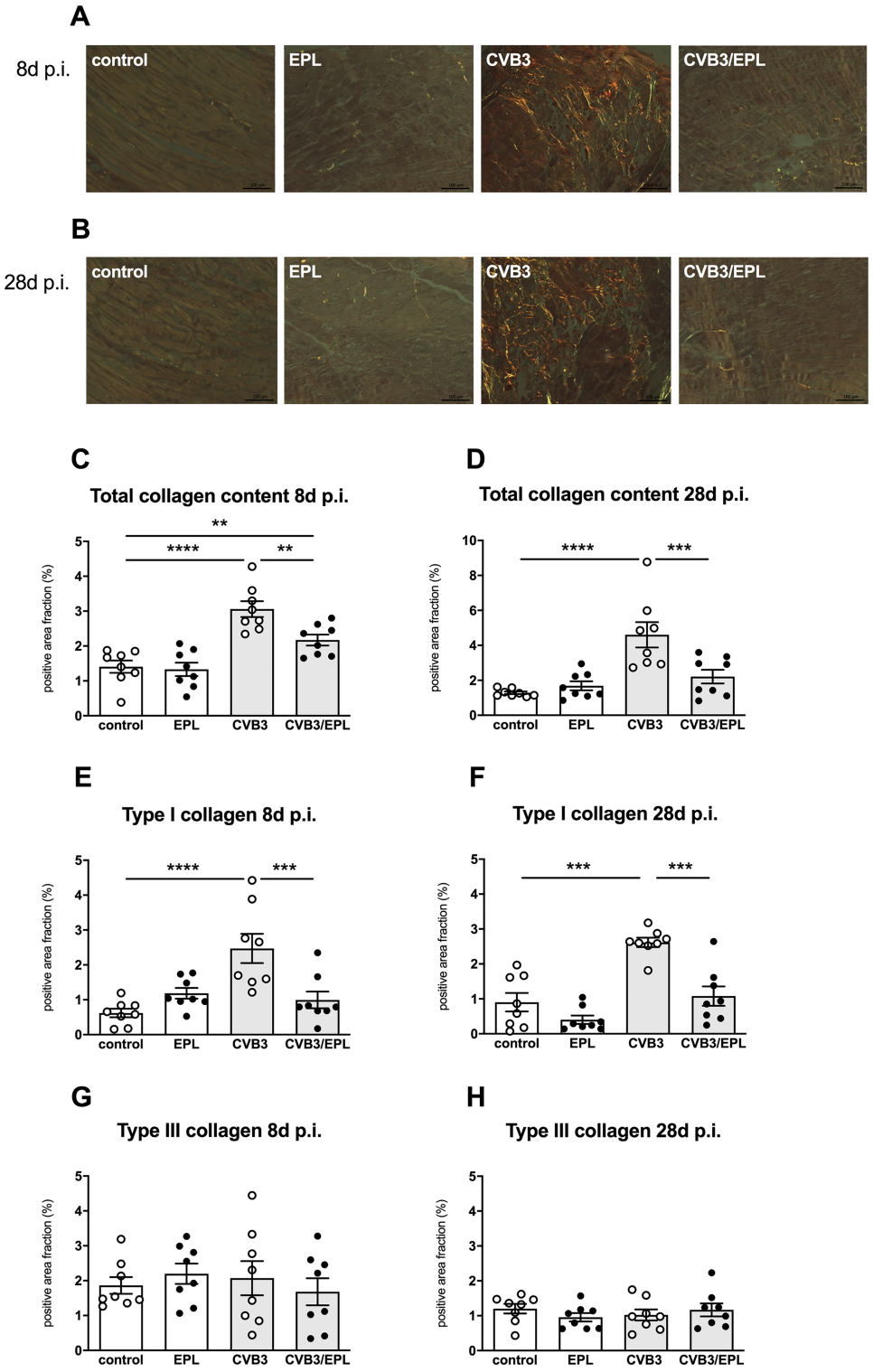

FIGURE 7 Collagen production is less pronounced in cardiac fibroblasts cultured with medium of coxsackievirus B3-infected HL-1 cardiomyocytes treated with eplerenone vs. medium of untreated coxsackievirus B3-infected HL-1 cardiomyocytes. Collagen production in cardiac fibroblasts is depicted as arbitrary units representing the absorbance of Sirius Red staining divided by the mean of the absorbance of crystal violet staining. Data are reported as mean ± SEM and were analysed with one-way ANOVA and Fisher's least significant difference (LSD) *post hoc* test (*$P < 0.05$; ****$P < 0.0001$ with $n = 11–12$/group). CVB3, coxsackievirus B3; EPL, eplerenone.

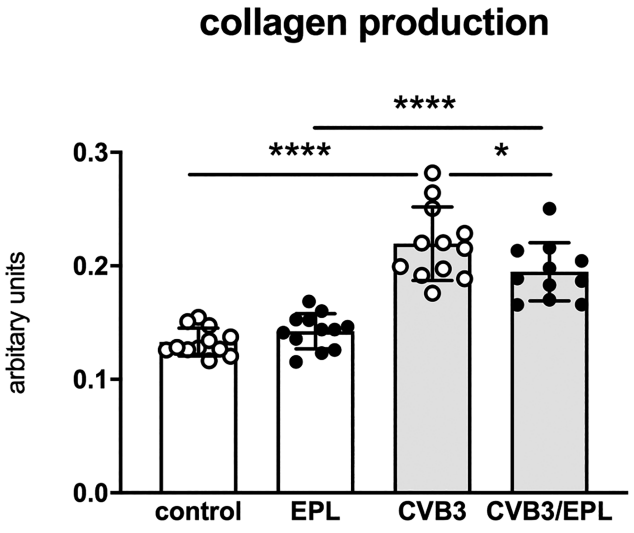

Eplerenone reduces the expression and activity of cardiac matrix metalloproteinases in coxsackievirus B3-induced myocarditis

Expression of MMP-3, MMP-8, MMP-12, and MMP-13 was evaluated by real-time PCR (*Figure* S2), while gelatinolytic activity of active MMP-2 and MMP-9 was measured by gelatin zymography (*Figure* 8). At Day 8 p.i., gene expression of MMP-3, MMP-8, MMP-12, and MMP-13 was higher than that of the control group (*Figure* S2). The tremendously enhanced expression of the collagenase MMP-8 is most likely due to infiltrating neutrophils, which are the primary source of MMP-8.[48] In parallel, the activity of MMP-2 and MMP-9 was increased in the heart of virus-treated mice vs. control animals at Day 8 p.i. (*Figure* 8). At Day 8 after CVB3 infection, a significant reduction of MMP-3, MMP-8, and MMP-12 mRNA levels as well as of MMP-2 and MMP-9 activity was observed in the CVB3/EPL group vs. CVB3 animals, respectively (*Figure* S2 and *Figure* 8). At 28 days post CVB3 infection, no changes were observed.

With respect to TIMP expression, only TIMP-1 was elevated in CVB3 mice vs. controls, whereas for TIMP-2 and TIMP-4, no changes were detected (*Figure* S3). EPL in CVB3-infected animals reduced mRNA levels of TIMP-1 and TIMP-2 compared with vehicle-treated CVB3 mice.

Discussion

The key finding in the current study is that an early intervention with the selective MRA EPL starting in the acute phase post CVB3 infection induced already favourable pleiotropic and immunomodulatory effects at Day 8 in a murine model of persisting CVB3-induced myocarditis, so that also in the long run, cardiac adverse remodelling and function were improved.

Human cardiac persistence of enteroviruses including CVB3 is associated with progression of LV dysfunction and a lack of clinical improvement.[6,49] An immunosuppressive intervention is not recommended under these conditions, and although pilot studies showed that in persisting infection a treatment with interferon-β can result in viral elimination and clinical improvement,[50,51] no anti-viral treatment is established until today.[1,52] Although 50% of infected patients eliminate enteroviruses spontaneously over the time,[49] a significant number of patients will suffer from the consequences of defect healing and adverse remodelling, which includes the development of myocarditis with preserved ejection fraction[53–55] or dilated cardiomyopathy with heightened risk of heart failure worsening, arrhythmias, and death.[13,54]

Because direct anti-viral strategies are not established[1] and aldosterone formation is increased in human acute myocarditis,[40] able to aggravate inflammatory and fibrotic effects, its inhibition might be an important strategy to reduce downstream complications. In non-myocarditis animal models, aldosterone inhibition was able to reduce myocardial ICAM-1 expression in conjunction with augmented infiltration/presence of monocytes/macrophages and induction of oxidative stress,[38] but it remained uncertain if a reduced infiltration of monocytes would be favourable in the context of viral myocarditis. Therefore, it is important to study if, and at what time point, an aldosterone-blocking intervention is effective and safe. According to the different time points and phases of the host immune and defence reaction, a CVB3 infection is conceptually divided into three distinct phases.[8] The first 3–4 days are the so-called acute phase, which is characterized by virus replication and the induction of the innate immune response. Virus-induced tissue damage[56] and recognition of viral pathogens contribute to an increased expression of pro-inflammatory cytokines like IL-1, IL-6, TNF-α, and interferons. These cytokine signals activate local macrophages and up-regulate ICAM-1 as well as chemokines for further recruitment of innate immune cells.[20,27,57] This is followed by a subacute phase, which occurs approximately from the fifth to 14th day, by which natural killer cells and monocytes are recruited for viral elimination or phagocytosis of dead cells, followed by cells of the adaptive immunity. During this phase, the immune response not only eliminates infected and dead cells but also significantly contributes to irreversible cardiac damage. At

FIGURE 8 Eplerenone decreases the activity of matrix metalloproteinase-2 and metalloproteinase-9 in coxsackievirus B3-induced myocarditis. Myocardial MMP-2 (A and B) and MMP-9 (C and D) activity measured by gelatin zymography at 8 (left panels) and 28 days (right panels) post infection. Quantitative analysis of the blots is depicted as bar graphs as well as a representative blot (E). MMP activities are expressed as fold changes normalized to the control group at Day 8 post infection. Data are reported as mean ± SEM and were analysed with one-way ANOVA and Fisher's least significant difference (LSD) *post hoc* test or Welch–ANOVA (*$P < 0.05$, **$P < 0.01$; ***$P < 0.001$; ****$P < 0.0001$ with n = 8/group). CVB3, coxsackievirus B3; d, days; EPL, eplerenone; p.i., post infection.

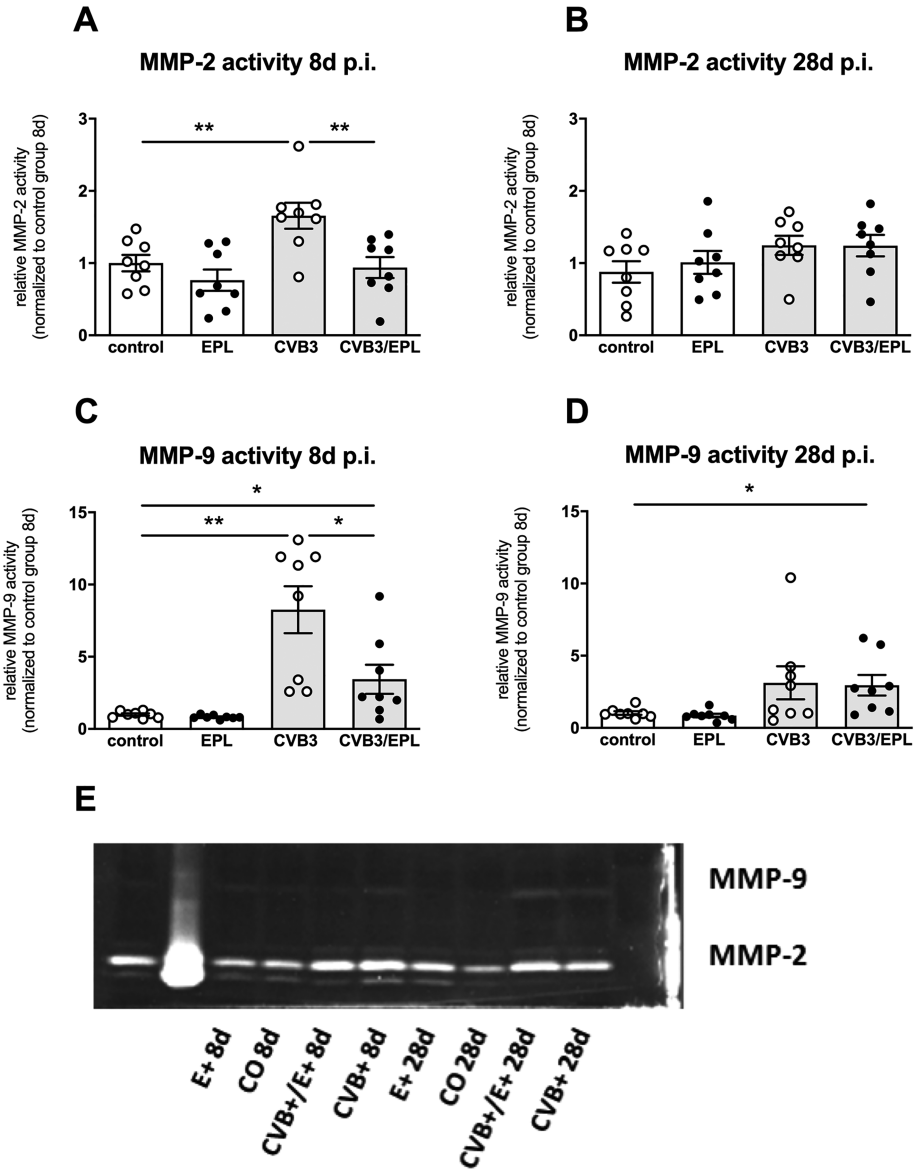

the fourth day, with a maximum at about the 14th day p.i., cardiac remodelling and fibrotic replacement start.[57]

We demonstrate in our study that an intervention with EPL starting at the acute phase and lasting until the fibrogenic phase exerted immunomodulatory, anti-oxidative, anti-apoptotic, and anti-fibrotic effects. We did not find a complete shutdown of the immunological defence reaction, as shown by no significant influence of EPL on the cardiac expression of pro-inflammatory cytokines (IL-6 and TNF-α). This indicates an immunomodulation rather than an immunosuppression, which is important, in the context of viral myocarditis. In addition, we observed a decrease of ICAM-1 expression and reduced recruitment/presence of monocytes/macrophages. The decreased infiltration/presence of monocytes/macrophages did not affect the viral load. Additionally, EPL therapy markedly

declined the increase of oxidative stress, as measured by nitrotyrosine staining. This is of particular importance because oxidative stress induces MMP transcription and additionally activates MMPs by posttranslational modification, thus causing an aggravation of the pre-existing MMP imbalance, inflammation, and fibrosis.[48,58] Moreover, oxidative stress[59] as well as aldosterone[60] is known to induce myocyte apoptosis, causing a further deterioration of LV function.[61] This assumption was confirmed by TUNEL assay, as we observed a decrease of apoptotic myocytes in CVB3-infected animals under EPL therapy and further supported by our *in vitro* findings, indicating a reduction in oxidative stress and apoptosis in CVB3-infected HL-1 cardiomyocytes treated with EPL vs. untreated CVB3-infected HL-1 cardiomyocytes. Furthermore, collagen production was less pronounced in cardiac fibroblasts cultured with medium of CVB3-infected HL-1 cardiomyocytes treated with EPL vs. untreated CVB3-infected HL-1, suggesting that the EPL-mediated protective effects on cardiomyocytes can influence cardiac fibroblast collagen production in a paracrine manner and includes modulation of the cardiomyocyte 'secretome'. This cardiomyocyte–cardiac fibroblast crosstalk is in agreement with observations from Rickard *et al*.[62] and Messaoudi *et al*.,[63] who demonstrated that aldosterone-induced signalling in cardiomyocytes is associated with cardiac fibrosis. With respect to ECM regulation in mice, we found an increase in cTGF and collagen I, but not collagen III,[64] as well as an increased expression and activity of collagenases (MMP-8 and MMP-13), gelatinases (MMP-2 and MMP-9), and stromelysins (MMP-3), while the expression of TIMP-1 through 4 was not significantly regulated. The result was a progressive cardiac fibrosis at Day 28, which was improved by early EPL treatment. Similar to the direct markers of inflammation, MMP activity was not decreased below control level, indicating that a certain minimal MMP activity is needed to maintain the integrity of the ECM.

Similar findings as presented here could also been seen in an encephalovirus myocarditis model, where an early (0th–7th day after infection) but not late (≥7th day after infection) intervention with EPL exerted anti-inflammatory and anti-fibrotic effects and improved mortality.[65] Interestingly, like in our study, these beneficial effects were independent of a reduction in viral load. This result implicates an important safety aspect, because, in contrast to steroid-based immunosuppressive strategies, EPL seems not to be associated with the risk of viral aggravation. Furthermore, the results of both animal studies suggest that the pleiotropic and immunomodulatory effects of EPL are independent of the viral type causing the myocarditis, because the common unspecific healing and defence response of the immune system is modulated, but not the direct anti-viral reaction. Hence, we suggest that MRA therapy may also be useful for COVID-19-associated myocarditis, because it has been shown that SARS-coronavirus 2-infected macrophages can also migrate into the heart.[5]

In summary, our study demonstrates that early treatment with MRA, starting at the acute phase of CVB3 infection, exerted pleiotropic, including immunomodulatory, antioxidative, and anti-apoptotic effects, leading to prevention of adverse cardiac remodelling and dysfunction without affecting viral load, in a murine model of persisting viral myocarditis. This makes EPL an ideal candidate for an acute treatment of myocarditis, beside heart failure treatment. However, current guidelines do not consider aldosterone antagonist therapy for acute myocarditis. This new therapeutic concept should be tested in a clinical trial, involving female and male patients. Especially, because beyond the relevance of gender on the immune system[31] and outcome[66] in inflammatory cardiomyopathy, also a sex-specific response to aldosterone receptor antagonism has been shown for experimental myocardial infarction.[67] It is likely also attractive for cardiac and non-cardiac inflammation-induced organ damage, including in COVID-19, because the described immunomodulatory effect of EPL was also found in a model of inflammatory lung disease.[68]

Acknowledgement

The authors thank Kerstin Puhl for excellent technical assistance.

Conflict of interest

C. T. and M. P. received speaker honoraria from Pfizer. S. D. A. reports receiving fees from Bayer, Boehringer Ingelheim, Cardiac Dimension, Impulse Dynamics, Novartis, Servier, St. Jude Medical, and Vifor Pharma; and grant support from Abbott Vascular and Vifor Pharma.

Funding

This study was supported by the Deutsche Forschungsgemeinschaft through SFB Transregio 19 (grant SFB Transregio 19 A2) and by research grants from Pfizer to C. T. and M. P.

Supporting information

Additional supporting information may be found online in the Supporting Information section at the end of the article.

Figure S1. Eplerenone attenuates left ventricular gene expression of fibrosis markers in Coxsackievirus B3-induced

myocarditis. Gene expression of Col1a1 (A+B), Col3a1 (C+D), connective tissue growth factor (cTGF; E+F), and transforming growth factor (TGF)-β (G+H) determined by real-time PCR at 8 days (left panels) and 28 days (right panels) after saline injection or CVB3 infection. Data are reported as mean±SEM and were analysed with One-way ANOVA and Fisher`s LSD post hoc test or Welch-ANOVA (*$P<0.05$; **$P<0.01$; ***$P<0.001$; ****$P<0.0001$ with n=7-8/group). *CVB3:* Coxsackievirus B3; *d:* days; *EPL*: Eplerenone; *p.i.* post infection.

Figure S2. Eplerenone reduces cardiac matrix metalloproteinases expression in Coxsackievirus B3-induced myocarditis. Myocardial matrix metalloproteinases (MMP)-3 (A+B), -8 (C +D), and -12 (E+F), -13 (G+H) mRNA expression at day 8 (left panel) and 28 days (right panel) after saline injection or CVB3 infection determined by real-time PCR. Data are reported as mean±SEM and were analysed with One-way ANOVA and Fisher`s LSD post hoc test or Welch-ANOVA (*$p<0.05$; **$P<0.01$; ***$P<0.001$; ****$P<0.0001$ with n=7-8/group). *CVB3:* Coxsackievirus B3; *d:* days; *EPL*: Eplerenone; *p.i.* post infection.

Figure S3. Eplerenone does not alter left ventricular expression of myocardial tissue inhibitors of metalloproteinases in Coxsackievirus B3-induced myocarditis. Gene expression of tissue inhibitor of metalloproteinases (TIMP)-1 (A+B), TIMP-2 (C+D), and TIMP-4 (E+F) determined by real-time PCR at 8 days (left panels) and 28 days (right panel) after saline injection or CVB3 infection. Data are reported as mean ±SEM and were analysed with One-way ANOVA and Fisher`s LSD post hoc test or Welch-ANOVA (*$P<0.05$; **$P<0.01$; ***$P<0.001$; ****$P<0.0001$ with n=7-8/group). *CVB3:* Coxsackievirus B3; *d:* days; *EPL*: Eplerenone; *p.i.* post infection.

References

1. Tschope C, Cooper LT, Torre-Amione G, Van Linthout S. Management of myocarditis-related cardiomyopathy in adults. *Circ Res* 2019; **124**: 1568–1583.
2. Trachtenberg BH, Hare JM. Inflammatory cardiomyopathic syndromes. *Circ Res* 2017; **121**: 803–818.
3. Heymans S, Pauschinger M, De Palma A, Kallwellis-Opara A, Rutschow S, Swinnen M, Vanhoutte D, Gao F, Torpai R, Baker AH, Padalko E, Neyts J, Schultheiss HP, Van de Werf F, Carmeliet P, Pinto YM. Inhibition of urokinase-type plasminogen activator or matrix metalloproteinases prevents cardiac injury and dysfunction during viral myocarditis. *Circulation* 2006; **114**: 565–573.
4. Rutschow S, Li J, Schultheiss HP, Pauschinger M. Myocardial proteases and matrix remodeling in inflammatory heart disease. *Cardiovasc Res* 2006; **69**: 646–656.
5. Tavazzi G, Pellegrini C, Maurelli M, Belliato M, Sciutti F, Bottazzi A, Sepe PA, Resasco T, Camporotondo R, Bruno R, Baldanti F, Paolucci S, Pelenghi S, Iotti GA, Mojoli F, Arbustini E. Myocardial localization of coronavirus in COVID-19 cardiogenic shock. *Eur J Heart Fail* 2020; **22**: 911–915.
6. Kuhl U, Pauschinger M, Noutsias M, Seeberg B, Bock T, Lassner D, Poller W, Kandolf R, Schultheiss HP. High prevalence of viral genomes and multiple viral infections in the myocardium of adults with "idiopathic" left ventricular dysfunction. *Circulation* 2005; **111**: 887–893.
7. Burch GE, Sun SC, Chu KC, Sohal RS, Colcolough HL. Interstitial and coxsackievirus B myocarditis in infants and children. A comparative histologic and immunofluorescent study of 50 autopsied hearts. *JAMA* 1968; **203**: 1–8.
8. Corsten MF, Schroen B, Heymans S. Inflammation in viral myocarditis: friend or foe? *Trends Mol Med* 2012; **18**: 426–437.
9. Van Linthout S, Stamm C, Schultheiss HP, Tschope C. Mesenchymal stem cells and inflammatory cardiomyopathy: cardiac homing and beyond. *Cardiol Res Pract* 2011; **2011**: 757154.
10. Spotnitz MD, Lesch M. Idiopathic dilated cardiomyopathy as a late complication of healed viral (Coxsackie B virus) myocarditis: historical analysis, review of the literature, and a postulated unifying hypothesis. *Prog Cardiovasc Dis* 2006; **49**: 42–57.
11. Cooper LT Jr, Keren A, Sliwa K, Matsumori A, Mensah GA. The global burden of myocarditis: part 1: a systematic literature review for the Global Burden of Diseases, Injuries, and Risk Factors 2010 study. *Glob Heart* 2014; **9**: 121–129.
12. Seferovic PM, Polovina M, Bauersachs J, Arad M, Gal TB, Lund LH, Felix SB, Arbustini E, Caforio ALP, Farmakis D, Filippatos GS, Gialafos E, Kanjuh V, Krljanac G, Limongelli G, Linhart A, Lyon AR, Maksimovic R, Milicic D, Milinkovic I, Noutsias M, Oto A, Oto O, Pavlovic SU, Piepoli MF, Ristic AD, Rosano GMC, Seggewiss H, Asanin M, Seferovic JP, Ruschitzka F, Celutkiene J, Jaarsma T, Mueller C, Moura B, Hill L, Volterrani M, Lopatin Y, Metra M, Backs J, Mullens W, Chioncel O, de Boer RA, Anker S, Rapezzi C, Coats AJS, Tschope C. Heart failure in cardiomyopathies: a position paper from the Heart Failure Association of the European Society of Cardiology. *Eur J Heart Fail* 2019; **21**: 553–576.
13. Ammirati E, Veronese G, Brambatti M, Merlo M, Cipriani M, Potena L, Sormani P, Aoki T, Sugimura K, Sawamura A, Okumura T, Pinney S, Hong K, Shah P, Braun O, Van de Heyning CM, Montero S, Petrella D, Huang F, Schmidt M, Raineri C, Lala A, Varrenti M, Foa A, Leone O, Gentile P, Artico J, Agostini V, Patel R, Garascia A, Van Craenenbroeck EM, Hirose K, Isotani A, Murohara T, Arita Y, Sionis A, Fabris E, Hashem S, Garcia-Hernando V, Oliva F, Greenberg B, Shimokawa H, Sinagra G, Adler ED, Frigerio M, Camici PG. Fulminant versus acute nonfulminant myocarditis in patients with left ventricular systolic dysfunction. *J Am Coll Cardiol* 2019; **74**: 299–311.
14. Esfandiarei M, McManus BM. Molecular biology and pathogenesis of viral myocarditis. *Annu Rev Pathol* 2008; **3**: 127–155.
15. Shanbhag SM, Greve AM, Aspelund T, Schelbert EB, Cao JJ, Danielsen R, Thornorgeirsson G, Sigurethsson S, Eiriksdottir G, Harris TB, Launer LJ, Guethnason V, Arai AE. Prevalence and prognosis of ischaemic and non-ischaemic myocardial fibrosis in older adults. *Eur Heart J* 2019; **40**: 529–538.
16. Tschope C, Van Linthout S, Spillmann F, Posch MG, Reinke P, Volk HD, Elsanhoury A, Kuhl U. Targeting CD20 + B-lymphocytes in inflammatory dilated cardiomyopathy with rituximab improves clinical course: a case series. *Eur Heart J Case Rep* 2019; **3**.
17. Jaquenod De Giusti C, Ure AE, Rivadeneyra L, Schattner M, Gomez

RM. Macrophages and galectin 3 play critical roles in CVB3-induced murine acute myocarditis and chronic fibrosis. *J Mol Cell Cardiol* 2015; **85**: 58–70.
18. Pappritz K, Savvatis K, Miteva K, Kerim B, Dong F, Fechner H, Muller I, Brandt C, Lopez B, Gonzalez A, Ravassa S, Klingel K, Diez J, Reinke P, Volk HD, Van Linthout S, Tschope C. Immunomodulation by adoptive regulatory T-cell transfer improves coxsackievirus B3-induced myocarditis. *FASEB J* 2018: fj201701408R.
19. Negrotto S, Jaquenod De Giusti C, Rivadeneyra L, Ure AE, Mena HA, Schattner M, Gomez RM. Platelets interact with coxsackieviruses B and have a critical role in the pathogenesis of virus-induced myocarditis. *J Thromb Haemost* 2015; **13**: 271–282.
20. Pappritz K, Savvatis K, Koschel A, Miteva K, Tschope C, Van Linthout S. Cardiac (myo)fibroblasts modulate the migration of monocyte subsets. *Sci Rep* 2018; **8**: 5575.
21. Lindner D, Li J, Savvatis K, Klingel K, Blankenberg S, Tschope C, Westermann D. Cardiac fibroblasts aggravate viral myocarditis: cell specific coxsackievirus B3 replication. *Mediators Inflamm* 2014; **2014**: 519528.
22. Savvatis K, Muller I, Frohlich M, Pappritz K, Zietsch C, Hamdani N, Grote K, Schieffer B, Klingel K, Van Linthout S, Linke WA, Schultheiss HP, Tschope C. Interleukin-6 receptor inhibition modulates the immune reaction and restores titin phosphorylation in experimental myocarditis. *Basic Res Cardiol* 2014; **109**: 449.
23. Kraft L, Erdenesukh T, Sauter M, Tschope C, Klingel K. Blocking the IL-1beta signalling pathway prevents chronic viral myocarditis and cardiac remodeling. *Basic Res Cardiol* 2019; **114**: 11.
24. Liao CW, Chou CH, Wu XM, Chen ZW, Chen YH, Chang YY, Wu VC, Rose-John S, Hung CS, Lin YH, Group TS. Interleukin-6 plays a critical role in aldosterone-induced macrophage recruitment and infiltration in the myocardium. *Biochim Biophys Acta Mol Basis Dis* 1866; **2020**: 165627.
25. Muller I, Pappritz K, Savvatis K, Puhl K, Dong F, El-Shafeey M, Hamdani N, Hamann I, Noutsias M, Infante-Duarte C, Linke WA, Van Linthout S, Tschope C. CX3CR1 knockout aggravates coxsackievirus B3-induced myocarditis. *PLoS ONE* 2017; **12**: e0182643.
26. Muller I, Vogl T, Pappritz K, Miteva K, Savvatis K, Rohde D, Most P, Lassner D, Pieske B, Kuhl U, Van Linthout S, Tschope C. Pathogenic role of the damage-associated molecular patterns S100A8 and S100A9 in coxsackievirus B3-induced myocarditis. *Circ Heart Fail* 2017; **10**.
27. Riad A, Westermann D, Escher F, Becher PM, Savvatis K, Lettau O, Heimesaat MM, Bereswill S, Volk HD, Schultheiss HP, Tschope C. Myeloid differentiation factor-88 contributes to TLR9-mediated modulation of acute coxsackievirus B3-induced myocarditis in vivo. *Am J Physiol Heart Circ Physiol* 2010; **298**: H2024–H2031.
28. Riad A, Westermann D, Zietsch C, Savvatis K, Becher PM, Bereswill S, Heimesaat MM, Lettau O, Lassner D, Dorner A, Poller W, Busch M, Felix SB, Schultheiss HP, Tschope C. TRIF is a critical survival factor in viral cardiomyopathy. *J Immunol* 2011; **186**: 2561–2570.
29. Tschope C, Muller I, Xia Y, Savvatis K, Pappritz K, Pinkert S, Lassner D, Heimesaat MM, Spillmann F, Miteva K, Bereswill S, Schultheiss HP, Fechner H, Pieske B, Kuhl U, Van Linthout S. NOD2 (nucleotide-binding oligomerization domain 2) is a major pathogenic mediator of coxsackievirus B3-induced myocarditis. *Circ Heart Fail* 2017; **10** (9): e003870.
30. Friebel J, Weithauser A, Witkowski M, Rauch BH, Savvatis K, Dorner A, Tabaraie T, Kasner M, Moos V, Bosel D, Gotthardt M, Radke MH, Wegner M, Bobbert P, Lassner D, Tschope C, Schutheiss HP, Felix SB, Landmesser U, Rauch U. Protease-activated receptor 2 deficiency mediates cardiac fibrosis and diastolic dysfunction. *Eur Heart J* 2019; **40**: 3318–3332.
31. Coronado MJ, Bruno KA, Blauwet LA, Tschope C, Cunningham MW, Pankuweit S, van Linthout S, Jeon ES, McNamara DM, Krejci J, Bienertova-Vasku J, Douglass EJ, Abston ED, Bucek A, Frisancho JA, Greenaway MS, Hill AR, Schultheiss HP, Cooper LT Jr, Fairweather D. Elevated sera sST2 is associated with heart failure in men </=50 years old with myocarditis. *J Am Heart Assoc* 2019; **8**: e008968.
32. Noguchi K, Tomita H, Kanayama T, Niwa A, Hatano Y, Hoshi M, Sugie S, Okada H, Niwa M, Hara A. Time-course analysis of cardiac and serum galectin-3 in viral myocarditis after an encephalomyocarditis virus inoculation. *PLoS ONE* 2019; **14**: e0210971.
33. Westermann D, Savvatis K, Lindner D, Zietsch C, Becher PM, Hammer E, Heimesaat MM, Bereswill S, Volker U, Escher F, Riad A, Plendl J, Klingel K, Poller W, Schultheiss HP, Tschope C. Reduced degradation of the chemokine MCP-3 by matrix metalloproteinase-2 exacerbates myocardial inflammation in experimental viral cardiomyopathy. *Circulation* 2011; **124**: 2082–2093.
34. Rutschow S, Leschka S, Westermann D, Puhl K, Weitz A, Ladyszenskij L, Jaeger S, Zeichhardt H, Noutsias M, Schultheiss HP, Tschope C, Pauschinger M. Left ventricular enlargement in coxsackievirus-B3 induced chronic myocarditis—ongoing inflammation and an imbalance of the matrix degrading system. *Eur J Pharmacol* 2010; **630**: 145–151.
35. Rude MK, Duhaney TA, Kuster GM, Judge S, Heo J, Colucci WS, Siwik DA, Sam F. Aldosterone stimulates matrix metalloproteinases and reactive oxygen species in adult rat ventricular cardiomyocytes. *Hypertension* 2005; **46**: 555–561.
36. Elsanhoury A, Tschope C, Van Linthout S. A toolbox of potential immune-related therapies for inflammatory cardiomyopathy. *J Cardiovasc Transl Res* 2020: 1–13.
37. Brilla CG, Weber KT. Reactive and reparative myocardial fibrosis in arterial hypertension in the rat. *Cardiovasc Res* 1992; **26**: 671–677.
38. Sun Y, Zhang J, Lu L, Chen SS, Quinn MT, Weber KT. Aldosterone-induced inflammation in the rat heart: role of oxidative stress. *Am J Pathol* 2002; **161**: 1773–1781.
39. Rocha R, Rudolph AE, Frierdich GE, Nachowiak DA, Kekec BK, Blomme EA, McMahon EG, Delyani JA. Aldosterone induces a vascular inflammatory phenotype in the rat heart. *Am J Physiol Heart Circ Physiol* 2002; **283**: H1802–H1810.
40. Cardona A, Baker P, Kahwash R, Smart S, Phay JE, Basso C, Raman SV. Evidence of aldosterone synthesis in human myocardium in acute myocarditis. *Int J Cardiol* 2019; **275**: 114–119.
41. Inciardi RM, Lupi L, Zaccone G, Italia L, Raffo M, Tomasoni D, Cani DS, Cerini M, Farina D, Gavazzi E, Maroldi R, Adamo M, Ammirati E, Sinagra G, Lombardi CM, Metra M. Cardiac involvement in a patient with coronavirus disease 2019 (COVID-19). *JAMA Cardiol* 2020.
42. Westermann D, Rutschow S, Jager S, Linderer A, Anker S, Riad A, Unger T, Schultheiss HP, Pauschinger M, Tschope C. Contributions of inflammation and cardiac matrix metalloproteinase activity to cardiac failure in diabetic cardiomyopathy: the role of angiotensin type 1 receptor antagonism. *Diabetes* 2007; **56**: 641–646.
43. Riad A, Jager S, Sobirey M, Escher F, Yaulema-Riss A, Westermann D, Karatas A, Heimesaat MM, Bereswill S, Dragun D, Pauschinger M, Schultheiss HP, Tschope C. Toll-like receptor-4 modulates survival by induction of left ventricular remodeling after myocardial infarction in mice. *J Immunol* 2008; **180**: 6954–6961.
44. Livak KJ, Schmittgen TD. Analysis of relative gene expression data using real-time quantitative PCR and the 2 (−delta delta C(T)) method. *Methods* 2001; **25**: 402–408.
45. Tschope C, Walther T, Koniger J, Spillmann F, Westermann D, Escher F, Pauschinger M, Pesquero JB, Bader M, Schultheiss HP, Noutsias M. Prevention of cardiac fibrosis and left ventricular dysfunction in diabetic cardiomyopathy in rats by transgenic expression of the human tissue kallikrein gene. *FASEB J* 2004; **18**: 828–835.
46. Pauschinger M, Knopf D, Petschauer S, Doerner A, Poller W, Schwimmbeck PL,

Kuhl U, Schultheiss HP. Dilated cardiomyopathy is associated with significant changes in collagen type I/III ratio. *Circulation* 1999; **99**: 2750–2756.
47. Savvatis K, van Linthout S, Miteva K, Pappritz K, Westermann D, Schefold JC, Fusch G, Weithauser A, Rauch U, Becher PM, Klingel K, Ringe J, Kurtz A, Schultheiss HP, Tschope C. Mesenchymal stromal cells but not cardiac fibroblasts exert beneficial systemic immunomodulatory effects in experimental myocarditis. *PLoS ONE* 2012; **7**: e41047.
48. Spinale FG. Myocardial matrix remodeling and the matrix metalloproteinases: influence on cardiac form and function. *Physiol Rev* 2007; **87**: 1285–1342.
49. Lassner D, Siegismund CS, Kuhl U, Rohde M, Stroux A, Escher F, Schultheiss HP. CCR5del32 genotype in human enteroviral cardiomyopathy leads to spontaneous virus clearance and improved outcome compared to wildtype CCR5. *J Transl Med* 2018; **16**: 249.
50. Schultheiss HP, Piper C, Sowade O, Waagstein F, Kapp JF, Wegscheider K, Groetzbach G, Pauschinger M, Escher F, Arbustini E, Siedentop H, Kuehl U. Betaferon in chronic viral cardiomyopathy (BICC) trial: effects of interferon-beta treatment in patients with chronic viral cardiomyopathy. *Clin Res Cardiol* 2016; **105**: 763–773.
51. Kuhl U, Pauschinger M, Schwimmbeck PL, Seeberg B, Lober C, Noutsias M, Poller W, Schultheiss HP. Interferon-beta treatment eliminates cardiotropic viruses and improves left ventricular function in patients with myocardial persistence of viral genomes and left ventricular dysfunction. *Circulation* 2003; **107**: 2793–2798.
52. Caforio AL, Pankuweit S, Arbustini E, Basso C, Gimeno-Blanes J, Felix SB, Fu M, Helio T, Heymans S, Jahns R, Klingel K, Linhart A, Maisch B, McKenna W, Mogensen J, Pinto YM, Ristic A, Schultheiss HP, Seggewiss H, Tavazzi L, Thiene G, Yilmaz A, Charron P, Elliott PM, European Society of Cardiology Working Group on M, Pericardial D. Current state of knowledge on aetiology, diagnosis, management, and therapy of myocarditis: a position statement of the European Society of Cardiology Working Group on Myocardial and Pericardial Diseases. *Eur Heart J* 2013; **34**: 2636–2648 48a-48d.
53. Kasner M, Aleksandrov A, Escher F, Al-Saadi N, Makowski M, Spillmann F, Genger M, Schultheiss HP, Kuhl U, Pieske B, Morris DA, Noutsias M, Tschope C. Multimodality imaging approach in the diagnosis of chronic myocarditis with preserved left ventricular ejection fraction (MCpEF): the role of 2D speckle-tracking echocardiography. *Int J Cardiol* 2017; **243**: 374–378.
54. Aquaro GD, Perfetti M, Camastra G, Monti L, Dellegrottaglie S, Moro C, Pepe A, Todiere G, Lanzillo C, Scatteia A, Di Roma M, Pontone G, Perazzolo Marra M, Barison A, Di Bella G. Cardiac Magnetic Resonance Working Group of the Italian Society of C. Cardiac MR with late gadolinium enhancement in acute myocarditis with preserved systolic function: ITAMY study. *J Am Coll Cardiol* 2017; **70**: 1977–1987.
55. Pieske B, Tschope C, de Boer RA, Fraser AG, Anker SD, Donal E, Edelmann F, Fu M, Guazzi M, Lam CSP, Lancellotti P, Melenovsky V, Morris DA, Nagel E, Pieske-Kraigher E, Ponikowski P, Solomon SD, Vasan RS, Rutten FH, Voors AA, Ruschitzka F, Paulus WJ, Seferovic P, Filippatos G. How to diagnose heart failure with preserved ejection fraction: the HFA-PEFF diagnostic algorithm: a consensus recommendation from the Heart Failure Association (HFA) of the European Society of Cardiology (ESC). *Eur J Heart Fail* 2020; **22**: 391–412.
56. Badorff C, Lee GH, Lamphear BJ, Martone ME, Campbell KP, Rhoads RE, Knowlton KU. Enteroviral protease 2A cleaves dystrophin: evidence of cytoskeletal disruption in an acquired cardiomyopathy. *Nat Med* 1999; **5**: 320–326.
57. Papageorgiou AP, Heymans S. Interactions between the extracellular matrix and inflammation during viral myocarditis. *Immunobiology* 2012; **217**: 503–510.
58. Westermann D, Savvatis K, Schultheiss HP, Tschope C. Immunomodulation and matrix metalloproteinases in viral myocarditis. *J Mol Cell Cardiol* 2010; **48**: 468–473.
59. Li X, Moody MR, Engel D, Walker S, Clubb FJ Jr, Sivasubramanian N, Mann DL, Reid MB. Cardiac-specific overexpression of tumor necrosis factor-alpha causes oxidative stress and contractile dysfunction in mouse diaphragm. *Circulation* 2000; **102**: 1690–1696.
60. De Angelis N, Fiordaliso F, Latini R, Calvillo L, Funicello M, Gobbi M, Mennini T, Masson S. Appraisal of the role of angiotensin II and aldosterone in ventricular myocyte apoptosis in adult normotensive rat. *J Mol Cell Cardiol* 2002; **34**: 1655–1665.
61. Kuster GM, Kotlyar E, Rude MK, Siwik DA, Liao R, Colucci WS, Sam F. Mineralocorticoid receptor inhibition ameliorates the transition to myocardial failure and decreases oxidative stress and inflammation in mice with chronic pressure overload. *Circulation* 2005; **111**: 420–427.
62. Rickard AJ, Morgan J, Bienvenu LA, Fletcher EK, Cranston GA, Shen JZ, Reichelt ME, Delbridge LM, Young MJ. Cardiomyocyte mineralocorticoid receptors are essential for deoxycorticosterone/salt-mediated inflammation and cardiac fibrosis. *Hypertension* 2012; **60**: 1443–1450.
63. Messaoudi S, Gravez B, Tarjus A, Pelloux V, Ouvrard-Pascaud A, Delcayre C, Samuel J, Launay JM, Sierra-Ramos C, de la Rosa A, Clement K, Farman N, Jaisser F. Aldosterone-specific activation of cardiomyocyte mineralocorticoid receptor in vivo. *Hypertension* 2013; **61**: 361–367.
64. Lang C, Sauter M, Szalay G, Racchi G, Grassi G, Rainaldi G, Mercatanti A, Lang F, Kandolf R, Klingel K. Connective tissue growth factor: a crucial cytokine-mediating cardiac fibrosis in ongoing enterovirus myocarditis. *J Mol Med (Berl)* 2008; **86**: 49–60.
65. Xiao J, Shimada M, Liu W, Hu D, Matsumori A. Anti-inflammatory effects of eplerenone on viral myocarditis. *Eur J Heart Fail* 2009; **11**: 349–353.
66. McNamara DM, Starling RC, Cooper LT, Boehmer JP, Mather PJ, Janosko KM, Gorcsan J 3rd, Kip KE, Dec GW, Investigators I. Clinical and demographic predictors of outcomes in recent onset dilated cardiomyopathy: results of the IMAC (Intervention in Myocarditis and Acute Cardiomyopathy)-2 study. *J Am Coll Cardiol* 2011; **58**: 1112–1118.
67. Kanashiro-Takeuchi RM, Heidecker B, Lamirault G, Dharamsi JW, Hare JM. Sex-specific impact of aldosterone receptor antagonism on ventricular remodeling and gene expression after myocardial infarction. *Clin Transl Sci* 2009; **2**: 134–142.
68. Lieber GB, Fernandez X, Mingo GG, Jia Y, Caniga M, Gil MA, Keshwani S, Woodhouse JD, Cicmil M, Moy LY, Kelly N, Jimenez J, Crawley Y, Anthes JC, Klappenbach J, Ma YL, McLeod RL. Mineralocorticoid receptor antagonists attenuate pulmonary inflammation and bleomycin-evoked fibrosis in rodent models. *Eur J Pharmacol* 2013; **718**: 290–298.